Brain-state–independent neural representation of peripheral stimulation in rat olfactory bulb

Anan Li[a,b], Ling Gong[a], and Fuqiang Xu[a,c,1]

[a]State Key Laboratory of Magnetic Resonance, Atomic and Molecular Physics, Wuhan Institute of Physics and Mathematics, Chinese Academy of Sciences, Wuhan 430071, China; [b]Department of Chemistry and Life Science, Hubei University of Education, Wuhan 430205, China; and [c]Division of Biomedical Photonics, Wuhan National Laboratory of Optoelectronics, Wuhan 430074, China

Edited* by Robert G. Shulman, Yale University School of Medicine, New Haven, CT, and approved January 21, 2011 (received for review September 15, 2010)

It is critical for normal brains to perceive the external world precisely and accurately under ever-changing operational conditions, yet the mechanisms underlying this fundamental brain function in the sensory systems are poorly understood. To address this issue in the olfactory system, we investigated the responses of olfactory bulbs to odor stimulations under different brain states manipulated by anesthesia levels. Our results revealed that in two brain states, where the spontaneous baseline activities differed about twofold based on the local field potential (LFP) signals, the levels of neural activities reached after the same odor stimulation had no significant difference. This phenomenon was independent of anesthetics (pentobarbital or chloral hydrate), stimulating odorants (ethyl propionate, ethyl butyrate, ethyl valerate, amyl acetate, n-heptanal, or 2-heptanone), odor concentrations, and recording sites (the mitral or granular cell layers) for LFPs in three frequency bands (12–32 Hz, 33–64 Hz, and 65–90 Hz) and for multiunit activities. Furthermore, the activity patterns of the same stimulation under these two brain states were highly similar at both LFP and multiunit levels. These converging results argue the existence of mechanisms in the olfactory bulbs that ensure the delivery of peripheral olfactory information to higher olfactory centers with high fidelity under different brain states.

The ability to perceive the ever-changing external world accurately and precisely is a basic brain function. It is critical for daily life, survival, and higher brain functions, such as making decisions, plans, and judgments. However, the brain itself operates in ever-changing states (1, 2) or baselines (3) that are constantly modulated by external and internal factors, such as physical, physiological, psychological, clinical, and metabolic conditions. Therefore, elucidation of how sensory systems represent the same sensory information to the brain under different operational states is fundamental to understanding the related brain functions (1, 4–6).

The olfactory system, as the most direct and intrinsic sensory module (1, 7, 8), provides a unique model to study the principles and functional mechanisms of the brain. The peripheral olfactory information takes just one synapse to enter the olfactory bulb (OB) in the brain. The OB outputs directly to the olfactory cortices that mostly belong to the limbic system. As a center to code and process the peripheral olfactory inputs and a hub to distribute the processed information to the olfactory cortices (9–11), the OB consists of laminar structures, from the outer surface to the inner core: the olfactory nerve, glomerular, external plexiform, mitral cell layer (MCL), and granular cell (GCL) layer. All peripheral olfactory input is received by a few thousand glomeruli, which generate an odor-specific spatiotemporal activity pattern across the glomerular layer (10, 12, 13). The information is mainly processed in the external plexiform layer that contains a dense dendrodendritic network formed between the secondary dendrites of the mitral/tufted (M/T) cells, whose somas are located in the MCL, and the dendrites of granular cells, whose somas are located in the GCL, then sent to higher olfactory centers by M/T cells (11, 14, 15). Under given conditions, the representation and process of the olfactory information in the OB and the regulation of OB activity by the other brain regions have been extensively studied, and have greatly advanced our understanding of the olfactory system (6, 16–18). However, how the OB processes, represents, and transmits information of the same olfactory stimulus in different brain states has not been systematically investigated (19–21).

In this study, we examined the OB activities at rest and after stimulation in different brain states. We found that in two resting states with rather different baseline activities, the levels of peak activities of the same stimulation had no significant difference. This phenomenon was observed for both local field potential (LFP) and multiunit activity, independent of anesthetics, stimulating odorants, odorant concentrations, and recording sites in the OB. These results suggest that in the OB, the same peripheral event is represented by a similar population of neurons with similar roles and activity levels, independent of brain states. We speculate that this invariability of neural activity and representation for a specific event can ensure the peripheral olfactory information is sent to the higher olfactory cortices with high fidelity in different operational states of the brain.

Results

Baseline LFP Signals in the GCL. In the OB, the LFP signals in different frequencies (Fig. 1*A*) have different origins, amplitudes, and functions (22–25). The GCL contains a large amount of local neurons whose dendrites radiate almost exclusively toward the more superficial external plexiform layer, generating the strongest LFP signals in the OB (24, 25). Comparing the high brain state (HBS) with the low brain state (LBS) generated by chloral hydrate, the baseline activities for all three LFP bands are significantly increased by about 50% (Fig. 1*B*). Because the baseline activities and the increases in HBS are band-specific (Fig. 1*A* and Table S1 for detailed statistics), all LFP and multiunit signals are normalized against these in HBS to represent the neuronal activity changes in different brain conditions.

Effects of Brain States on GCL Responses. When the animal was stimulated with amyl acetate, the neuronal activity was enhanced in both LBS and HBS. Although the baseline activities are significantly different, the activity levels reached for a given frequency band in LBS and HBS are similar (Fig. 1*A*). The time courses show some band-specific features. For example, the highest frequency band has the smallest activity increase and slowest recovering kinetics (Fig. 1*B*). However, statistical analyses reveal that there is no significant difference between the maximum LFP signals in LBS and HBS for a given band (Fig. 1*C*

Author contributions: A.L. and F.X. designed research; A.L. and L.G. performed research; A.L. and L.G. analyzed data; and A.L. and F.X. wrote the paper.

The authors declare no conflict of interest.

*This Direct Submission article had a prearranged editor.

Freely available online through the PNAS open access option.

[1]To whom correspondence should be addressed. E-mail: fuqiang.xu@wipm.ac.cn.

This article contains supporting information online at www.pnas.org/lookup/suppl/doi:10.1073/pnas.1013814108/-/DCSupplemental.

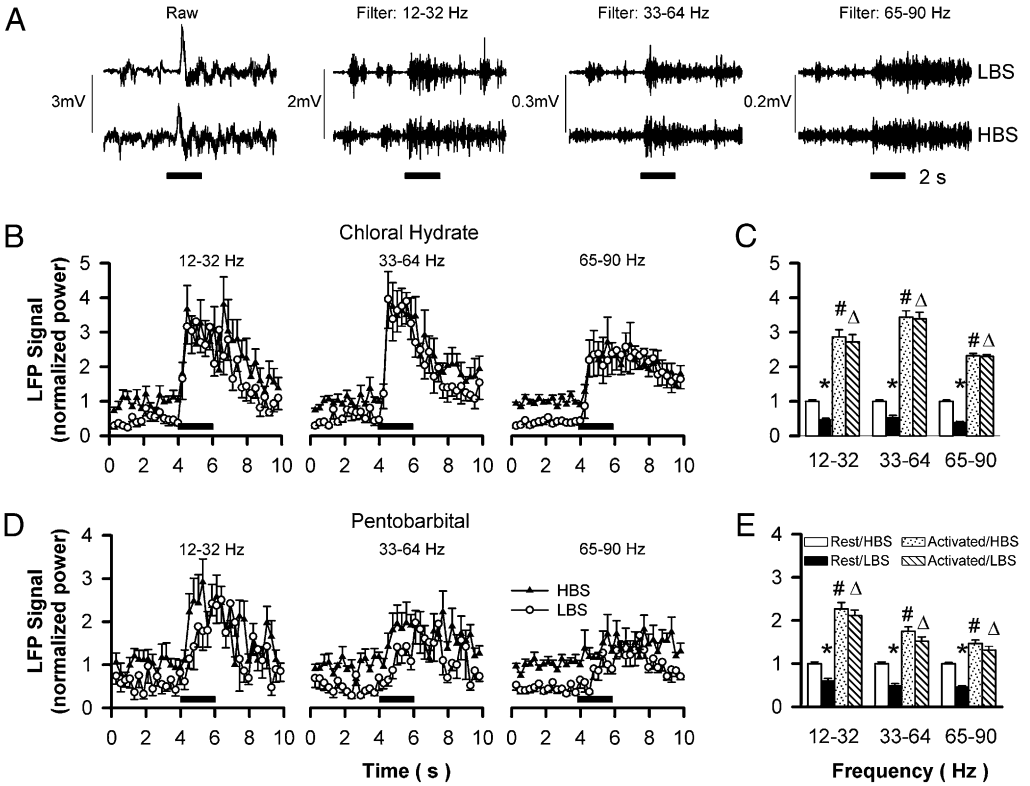

Fig. 1. LFP signals in the GCL under different brain states generated by different anesthetics. (*A*) LFP signals in three frequency bands were separated from the raw data in LBS and HBS (*Upper* and *Lower*). (*B* and *D*) The averaged time courses of LFP signals in the GCL for the three bands with chloral hydrate (n = 12) and pentobarbital (n = 13) as anesthetics, respectively. (*C* and *E*) Statistical analyses of the data in *B* and *D*, respectively. *HBS vs. LBS at rest; #rest vs. stimulated in HBS; Δrest vs. stimulated in LBS; $P < 0.001$ for all comparisons; no significant differences between the peak activities in LBS and HBS for any bands any anesthetic.

and Table S1), indicating that peak neuronal activity of a given event is independent of brain state.

Effects of Anesthetics on GCL Responses. Different anesthetics exert differential effects via distinct mechanisms (26). To test whether the observed phenomenon above is anesthetic specific, we examined the LFP signals with a different anesthetic in the same OB layer. Chloral hydrate targets both glycine and $GABA_A$ receptors, but pentobarbital targets only the $GABA_A$ receptor and, furthermore, with different subunit compositions targeted by chloral hydrate (27). In the LBS and HBS generated by pentobarbital similar to those by chloral hydrate, some anesthetic-specific effects are revealed, including smaller activity increases and slower rising rates after odor stimulation for all frequency bands. However, the peak activities elicited by the same stimulus are not significantly different, as in the case of chloral hydrate (Fig. 1 *D* and *E*, and Table S1), indicating that the observed phenomenon above is independent of anesthetics.

Effects of Brain States on the LFP Signals and Representations of Different Odors. It is generally accepted that a given olfactory stimulation elicits a specific activity pattern in the OB (12, 13, 28). To test whether the observed phenomenon above is odor-specific, we examined the GCL responses to five other odors at nine recording sites. Although Fig. 2*A* shows odor-specific responses at one site during one exposure, statistical analyses revealed that the activity pattern of each odor, formed by the LFP signals across all sites, is odor-specific (Fig. 2*B* and Table S2), and that the activity pattern of each site, formed by the LFP signals of all odorants, is site-specific (Fig S1 and Table S3). Interestingly, the activities in the LBS and HBS have no significant difference for a given odor at a given site, indicating that the phenomenon of brain-state–independent representation is not odor-specific (43 of 45 pairs) (Table S4). Because the activity at each point is highly similar under LBS and HBS, the corresponding two activity patterns of an odorant have no significant difference ($P < 0.005$ for all five odors, Fig. 2*B* and Table S3).

Effects of Odor Concentration on GCL Responses. Although the nominal concentration used above for all odorants is the same, 9.1% of the air stream flowing over pure odorants, the actual concentration is different because of the very different vapor pressures of these odorants. To assure that the observed phenomenon is not concentration-specific, LFP signal in the GCL elicited by different concentrations were recorded (Fig. 3). The signals of all LFP bands are significantly correlated with odor concentrations under both LBS and HBS ($P < 0.01$) (Table S5). More interestingly, the peak activities after stimulation under LBS and HBS in any of the frequency bands and concentrations are not significantly different ($P > 0.05$) (Table S5), indicating that the brain-state–independent representation is not concentration-specific.

Effects of Brain States on MCL Responses. Different bulbar layers have different cellular compositions and functions (11). The MCL contains M/T cell bodies and granular cell dendrites that are perpendicular to the layer, thus also generating strong LFP signals in both the LBS and HBS (Fig. 4 *A* and *B*, *Top*). In the same conditions as in Fig. 1*B*, the time courses show that different bands had different activation rates (Fig. 4*C*). Although some layer-specific properties are revealed, including smaller activity increases, and slower rising and recovering rates in the

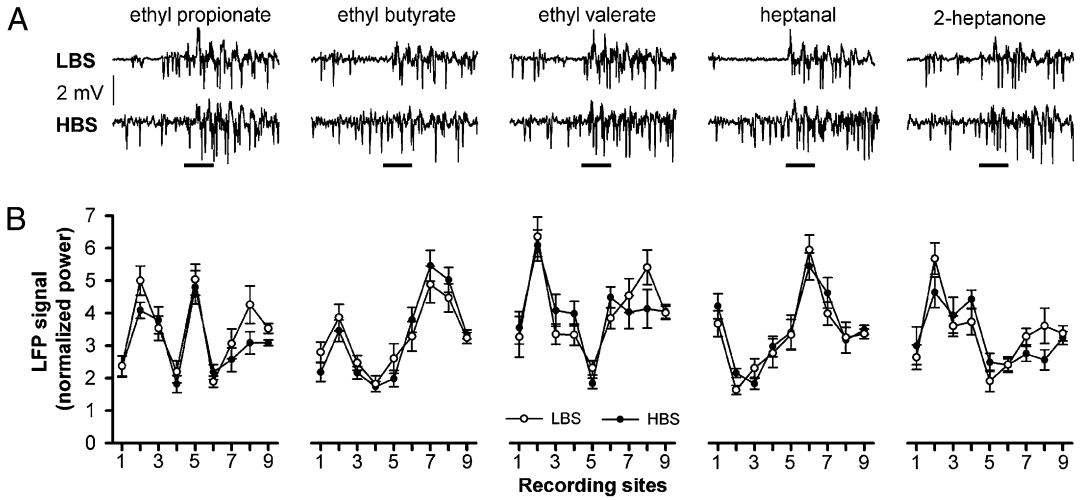

Fig. 2. The LFP signals of different odorants at different recording sites in LBS and HBS. (*A*) Raw LFP signals at recording site three elicited by five odorants with 2-s stimulation. (*B*) The LFP signals of the five odorants corresponding to *A* at nine recording sites. None of the pattern pairs for a given odorant in LBS and HBS is significantly different ($P < 0.02$) (Table S2).

MCL for all bands (Figs. 1*B* vs. 4*C*), there is no significant difference between the maximum LFP signals in the LBS and HBS for a given band, similar to the case of GCL (Fig. 4*D* and Table S1).

Effects of Brain States on Multiunit Activity. LFP is the integrated result of neural assembly near the recording electrode. However, a brain-state–independent LFP signal does not necessarily imply that the neurons in that assembly generate action potentials similarly after odor stimulation in different brain states. To clarify this theory, we analyzed the data from the same electrical recoding sites in the MCL to separate multiunit spiking signals, and found that the spiking rates are different at rest but similar after stimulation (Fig. 4 *A* and *B*, *Bottom*). The time courses show that the multiunit activity in LBS is more significantly suppressed at rest than all LFP bands. However, the spiking rates elicited by the same stimulation in LBS and HBS have no significant difference (Fig. 4*E*, *Inset*), similar to the case of LFP. Furthermore, the LFP signal and spiking activity in the MCL correlate well (Fig. 4*F*) ($P < 0.02$ for the three bands).

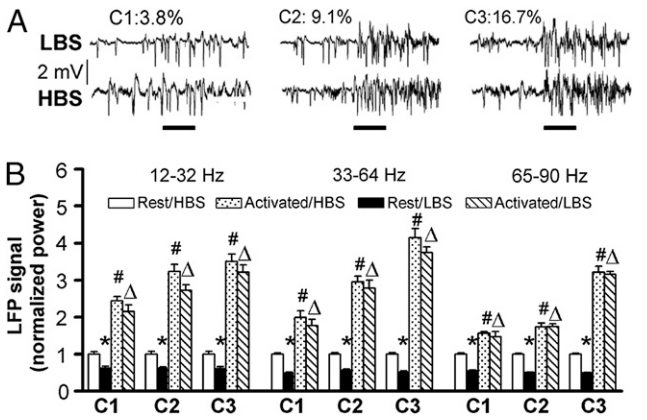

Fig. 3. The effects of odor concentration on the LFP signals in LBS and HBS. (*A*) Raw LFP signals at three concentrations with 2-s stimulation in LBS (*Upper*) and HBS (*Lower*). (*B*) Statistical analyses of the LFP signals in three frequency bands; the LFP signals are significantly correlated with concentration. *, #, and Δ, are the same as in Fig. 1; $P < 0.02$ for all comparisons; no significant difference between the peak activities in LBS and HBS for all three bands at all three concentrations ($n = 14$) (Table S5).

Effects of Brain States on the Representation of a Given Stimulus. The state-independent multiunit spiking activity implies that the neurons around the recording electrodes generate similar numbers of action potentials after odor stimulation in different brain states. The activity does not necessarily mean that these individual neurons act similarly. More detailed data analysis reveals that compared with HBS, neurons tend to fire less frequently in LBS (Fig. 4*G*), leading to different distribution patterns at rest (Pearson correlation $r_{\text{HBS vs. LBS}} = 0.43$; $P = 0.16$). After odor stimulation, neurons tend to fire at higher frequency, decreasing the number of neurons with a low firing rate and generating significantly different distribution patterns (rest vs. activated, $P = 0.78$ and 0.15 for LBS and HBS, respectively). More intriguingly, the two distribution patterns of HBS and LBS after odor stimulation are rather similar ($P = 0.002$), indicating that the peripheral olfactory information sent to the higher olfactory cortices after being processed in the OB is essentially independent of brain states.

Discussion

State-Independent LFP Signals for a Given Olfactory Stimulation. Our data showed that in different brain states manipulated by anesthesia depth, the baseline neuronal activities in the OB had a twofold difference, but the absolute neuronal activities elicited by the same olfactory stimulus were almost identical. This phenomenon of invariable neuronal activity for a given event was observed for LFP signals and multiunit spiking, elicited by different odorants and concentrations, recorded at different sites under different anesthetics. It has been shown that under the same anesthesia level (or brain state), the brain can switch between slow and fast wave states (19, 21). The higher cortex changes their responses to the same peripheral stimulation accordingly, but the OB does not, also indicating that the OB has its own mechanisms to maintain its responses independent of brain states.

This phenomenon of state-independent neuronal activity for a given event revealed here in the olfactory system has been observed in visual and somatosensory systems. In the primary visual cortex, the baseline activities can be manipulated, for example, with eyes open or closed in a dark room (29). Functional MRI has revealed that there is no significant difference between the peak activation levels for these different resting conditions

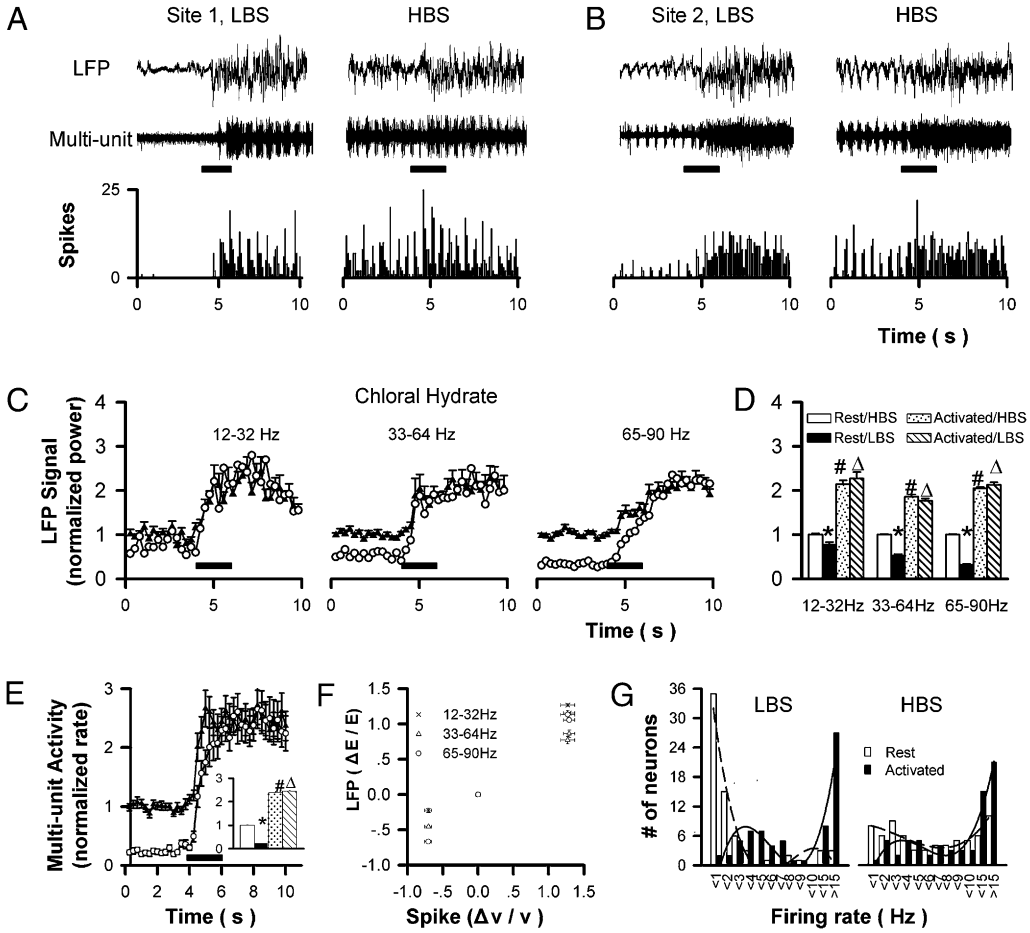

Fig. 4. Electrical recording in the MCL under LBS and HBS. (*A* and *B*) LFP signals (*Top*), multiunit spiking (*Middle*), and histogram of spiking (*Bottom*) at two recording sites with 2-s stimulation in LBS and HBS. (*C*) The averaged time courses of LFP signals in three bands (29 recording sites from 19 rats). (*D*) The statistical comparisons of data in *C*. (*E*) Multiunit signals and the statistical analyses. (*F*) Correlation between LFP and multiunit signals. (*G*) The distribution patterns of firing rate at rest and after stimulation in LBS and HBS, respectively; the last three bars were the number of neurons with firing frequency from 11 to 15, and > 15, respectively. *, #, and Δ are the same as in Fig. 1; $P < 0.001$ for all situations; no significant difference between the peak activities in LBS and HBS for all three LFP bands and multiunit signals; circles and filled circles in *C* and *E* are LBS and HBS, respectively.

when the same visual stimulus is presented (29, 30). By using anesthetics to alter the baseline activity to a broader range, multiunit spiking rates in the primary somatosensory cortex during forepaw stimulation are also independent of the baseline levels (31–33). The state-independent total neuronal activity described above, however, is not always observed, as the responses under deeper anesthesia are stronger in many reports (33–36), but weaker in some others (37–39). These differences might be a result of differences in experimental conditions (anesthetics, dosages, animals, and so forth), or studied regions (primary or higher cortices in the sensory systems).

It has been reported that in the aspects of LFP signals and spiking rates, task-related learning processes can modify the neural representation (40, 41). However, the objective modulation does not contradict the results in this study, because the task-related modified representations are also stable after the animals learned the task (40). Therefore, the modification just redefines the stimulus to generate a new representation and perception accordingly, conferring the system with higher efficiency for complex olfactory functions. It will be interesting to test whether the modified representation after task-related learning is also brain-state–independent (e.g., fed vs. fasted).

Neuronal Basis for the Larger Increment at LBS in the OB. The state-independent neuronal activity and representation for a given stimulus means that the increment is larger at LBS. The peripheral and centrifugal inputs and the intrinsic circuits together decide the OB activity. Although the effect of anesthesia on the peripheral inputs is negligible (42), it is more significant for the central processes (1, 19). The OB receives modulatory inputs from several nuclei (16–18, 43) and heavy feedback inputs from many cortices (11, 43, 44). Because multiple receptor types of these pathways spread over the OB, the effect of anesthesia on modulatory inputs is difficult to predict. However, with glutamate as a neurotransmitter, the feedback inputs are suppressed by anesthesia (6). Because their targets are the granular cells, the LBS will disinhibit the dendrodendritic network in the external plexiform layer, enhancing the activity increment.

Energetic Basis for the Enhanced Responses at LBS. The human brain makes up 2% of body mass, but consumes 20% of the cardiac output in adults and even more in babies (45, 46). Although blood supply to a given brain region can increase significantly during activation (3, 47, 48), the total amount to the brain is increased only slightly, even when the brain is performing difficult tasks (45, 46, 49). Therefore, even in a "rest" state, the brain needs large amounts of energy, close to its maximum quota. As revealed by comprehensive magnetic resonance spectroscopy studies, these energies are predominantly (>80%) used for neural activity (50, 51). The constraint of global energy avail-

ability in the brain would limit the total brain activity and determine how the brain performs its functions, as shown in ever-increasing studies that the two major systems in the brain for internal and external worlds cannot be activated simultaneously (52, 53). At the level of individual neurons, the same olfactory stimulation elicited stronger responses from M/T cells in anesthetized rats (19). This so-called "sparse coding" in the awake state, a mode taking advantage of timing to save energy, has been observed in several sensory systems (54, 55). In LBS, inhibition is stronger and the energy restrain is weaker, and the enhanced activity increment might be a balanced result. The energy restriction, combined with the interactions among the involved neuro-circuits discussed above, could lead to the observed larger increment in enhanced responses under LBS in the early sensory stages, although additional mechanisms are also likely involved.

Similarity of Activity Patterns Under Different Brain States. For the same olfactory stimulus, the activity patterns under LBS and HBS are highly similar on the levels of both LFP, which reflects the activity of many neurons close to the electrodes, and multiunit spiking, which reflects the activity of a few individual neurons (Figs. 2*B* and 4*G*). Furthermore, the LFP and multiunit spiking signals are well correlated, as shown in Fig. 4*F*. These coherent results indicate that in different brain states, the neurons in the OB activated by a given stimulus consist of similar populations with similar activities. In other words, under different brain states the same information is processed similarly in the OB, and the information sent to high olfactory cortices is also highly similar, as indicated by the highly similar patterns of multiunit activity (11, 15, 28, 56). For the same odor at different concentrations under the same brain state, previous studies using a variety of methods have revealed that their patterns have similar topography, but with concentration-correlated intensities (13, 57–60), leading to the speculation that the pattern topograpy represents stimulation quality and the intensity represents strength (13). The results in this study revealed that the intensity not only correlated with concentration (Fig. 3), but can vary with brain states. However, the total activity for a given stimulus is invariable in different brain states, consistent with the speculation that the total activity represents the event itself (61). However, the neurochemical and neurophysiological basis for these observations are barely known. Revelation of these mechanisms will be helpful in elucidating how the OB processes peripheral information and presents the processed information to higher stages.

Summary. The sensory systems should provide accurate information about the environment to the brain, and the brain has to form accurate perceptions from the input sensory information, independent of brain states. Our results showed that in the OB, the total activity elicited by the same odor stimulation was independent of global brain states, suggesting that the OB requires total, not incremental, neuronal activity to code, process, and convey the related sensory information. Furthermore, the activity patterns elicited by the same stimulus under different brain states were highly similar at both LFP and spiking levels, suggesting that similar populations of neurons are involved, each with similar roles and firing properties. This brain-state–independent neural activity and representation might be the mechanisms for the OB to present the peripheral olfactory information with high fidelity to the higher brain centers under ever-changing operational states.

Materials and Methods

Animal Surgery. All animal procedures were approved by the Chinese Academy of Sciences. Adult Sprague-Dawley rats (200–300 g) were anesthetized with intraperitoneal chloral hydrate (35 mg/kg), or pentobarbital (1 mg/kg). The rat was on a heat blanket and the core temperature was maintained at a constant (36 ± 1 °C) throughout the studies. Respiration was monitored with a piezoelectric device recording the chest wall movements.

Manipulation of Brain States. To reveal how the OB responds to odor stimulation under different brain states, we had to generate two levels of baseline activity reliably. Anesthetics, broadly used to alter global brain activity and baseline metabolism (26), are suitable for this purpose. After animal surgery and the placement of electrodes were finished, a supplementary dosage (30% of the original) was applied so both LFP and EEG recordings showed iso-electrical patterns (Fig. S2*A*). This deep anesthesia level was defined as LBS. The anesthesia level became lighter with time, so both LFP and EEG recordings showed more high-frequency signals (Fig. S2*B*). The lighter anesthesia level, at which the total LPF power was increased by 100 ± 10% compared with LBS, was defined as HBS. The time required to reach HBS was animal-dependent, but it generally took about 45 min. For pentobarbital, supplementary dosage (30% of the original) was applied to induce LBS. The HBS, which also had a 100% ± 10% increase of LFP signal compared with LBS, was generally reached about 30 min later.

Odor and Its Delivery. To reveal the representation of different odors in the OB under different brain states, amyl acetate, ethyl acetate, ethyl butyrate, ethyl valerate, heptanal, and 2-heptanone were selected based on the facts that their specific activity patterns overlap significantly in the general regions (where recordings were made in this article) in the middle-posterior area of medial side or the middle area of the lateral side of the OB (http://gara.bio.uci.edu/odorants.jsp?start=1&end=1&action=null and http://senselab.med.yale.edu/OdorMapDB/search.aspx for 2-deoxyglucose and functional MRI, respectively). The odorants were delivered to freely breathing animals by passing a stream of charcoal-filtered, humidified air over pure odorants, then diluted to one-tenth by an olfactometer. Different dilution ratios were used for concentration effects. Odor stimulation, triggered by the recording program, lasted for 2 s with an interstimulation interval >100 s to prevent habituation and a flow rate of 1 L/min.

LFP and Multiunit Recordings. Electrophysiological signals were used as an indicator of neuronal activity. The rat was placed prone on a stereotaxic holder on a vibration-free table inside a Faraday cage. After the skull over the OB was exposed and covered with mineral oil to prevent drying, microelectrode (~1-μm tip diameter tungsten with impedance of 2–4 MΩ; FHC) was inserted using a stereotaxic micromanipulator (Stoelting) to the GCL or MCL for recoding. Within the general recording regions (±1.5 mm lateral to midline, −7.0 mm anterior to Bregma), responses to all selected odorants can be readily obtained. The recording site was identified by histology after the experiments (*SI Text* and Fig. S3). A steel screw was fixed on the parietal lobe (±2.5 mm from midline, 4 mm posterior to Bregma) to record EEG signals. The LFP and EEG signals were amplified (×2,000; Dagan) before digitization (μ-1401; CED). The raw recording data were separated into LFP and multiunit signals (0.1–300 Hz and 300–3,000 Hz, respectively). At each recording site for each brain condition, four to six repeats were performed.

Data Process. Off-line analysis (Spike-2; CED) was used to create a spike template that was then used to create a temporal history of the ensemble by converting to spiking frequency (ν) with 0.256-s bins. The datasets in which excitatory multiunit spiking was not identified after odor stimulation under deep anesthesia were excluded for further data analysis. Spike analysis from 29 recording sites identified 69 individual neurons in the neuronal ensemble (*SI Text*). Raw data 4 s before and 6 s after the onset of the odor stimulus were selected for the processing of both LFP and multiunit signals, with the former period as the baseline and the latter as the activated. These 10-s data were binned with a width of 0.256 s (512 sample points for LFP). Time courses of LFP, multiunit, or spiking rate were obtained for each recording. Spectrum analysis and calculation of the spectrum power of LFP and the count of multiunit spikes were both performed using spike software (Spike-2; CED). After time-frequency transformation analysis of the LFP, three frequency bands of LFP, 12 to 32 Hz, 33 to 64 Hz, and 65 to 90 Hz, were filtered for further process. Student *t* test comparisons between resting and stimulated data were used to calculate significance of change. Pearson correlation coefficients are used to reflect the relationship between the activities obtained under different conditions, including recording sites, odorants, concentrations, brain conditions, and LFP and multiunit signals.

ACKNOWLEDGMENTS. We thank Nancy Xu of Barnard College for editing the manuscript. This work was supported in part by grants from the Natural National Science Foundation of China (C010607 and 20921004), the Chinese Academy of Sciences (08B1021001), the Wuhan National Laboratory of Optoelectronics (Z08004), and the Wuhan Institute of Physics and Mathematics (08K1011001).

1. Fontanini A, Katz DB (2008) Behavioral states, network states, and sensory response variability. *J Neurophysiol* 100:1160–1168.
2. van Eijsden P, Hyder F, Rothman DL, Shulman RG (2009) Neurophysiology of functional imaging. *Neuroimage* 45:1047–1054.
3. Shulman RG, Rothman DL, Hyder F (2007) A BOLD search for baseline. *Neuroimage* 36: 277–281.
4. Gaese BH, Ostwald J (2001) Anesthesia changes frequency tuning of neurons in the rat primary auditory cortex. *J Neurophysiol* 86:1062–1066.
5. Jermakowicz WJ, Casagrande VA (2007) Neural networks a century after Cajal. *Brain Res Brain Res Rev* 55:264–284.
6. Tsuno Y, Kashiwadani H, Mori K (2008) Behavioral state regulation of dendrodendritic synaptic inhibition in the olfactory bulb. *J Neurosci* 28:9227–9238.
7. Fontanini A, Bower JM (2006) Slow-waves in the olfactory system: An olfactory perspective on cortical rhythms. *Trends Neurosci* 29:429–437.
8. Shepherd GM (2005) Perception without a thalamus how does olfaction do it? *Neuron* 46:166–168.
9. Gottfried JA (2006) Smell: Central nervous processing. *Adv Otorhinolaryngol* 63: 44–69.
10. Ma M (2007) Encoding olfactory signals via multiple chemosensory systems. *Crit Rev Biochem Mol Biol* 42:463–480.
11. Shipley MT, Ennis M (1996) Functional organization of olfactory system. *J Neurobiol* 30:123–176.
12. Xu F, Greer CA, Shepherd GM (2000) Odor maps in the olfactory bulb. *J Comp Neurol* 422:489–495.
13. Xu F, Kida I, Hyder F, Shulman RG (2000) Assessment and discrimination of odor stimuli in rat olfactory bulb by dynamic functional MRI. *Proc Natl Acad Sci USA* 97: 10601–10606.
14. Schoppa NE, Urban NN (2003) Dendritic processing within olfactory bulb circuits. *Trends Neurosci* 26:501–506.
15. Wilson RI, Mainen ZF (2006) Early events in olfactory processing. *Annu Rev Neurosci* 29:163–201.
16. Petzold GC, Hagiwara A, Murthy VN (2009) Serotonergic modulation of odor input to the mammalian olfactory bulb. *Nat Neurosci* 12:784–791.
17. Shea SD, Katz LC, Mooney R (2008) Noradrenergic induction of odor-specific neural habituation and olfactory memories. *J Neurosci* 28:10711–10719.
18. Wilson DA (2009) Olfaction as a model system for the neurobiology of mammalian short-term habituation. *Neurobiol Learn Mem* 92:199–205.
19. Murakami M, Kashiwadani H, Kirino Y, Mori K (2005) State-dependent sensory gating in olfactory cortex. *Neuron* 46:285–296.
20. Rinberg D, Koulakov A, Gelperin A (2006) Sparse odor coding in awake behaving mice. *J Neurosci* 26:8857–8865.
21. Wilson DA (2010) Single-unit activity in piriform cortex during slow-wave state is shaped by recent odor experience. *J Neurosci* 30:1760–1765.
22. Bathellier B, Lagier S, Faure P, Lledo PM (2006) Circuit properties generating gamma oscillations in a network model of the olfactory bulb. *J Neurophysiol* 95:2678–2691.
23. Galán RF, Fourcaud-Trocmé N, Ermentrout GB, Urban NN (2006) Correlation-induced synchronization of oscillations in olfactory bulb neurons. *J Neurosci* 26:3646–3655.
24. Neville KR, Haberly LB (2003) Beta and gamma oscillations in the olfactory system of the urethane-anesthetized rat. *J Neurophysiol* 90:3921–3930.
25. Rojas-Líbano D, Kay LM (2008) Olfactory system gamma oscillations: The physiological dissection of a cognitive neural system. *Cogn Neurodyn* 2:179–194.
26. Gyulai FE (2004) Anesthetics and cerebral metabolism. *Curr Opin Anaesthesiol* 17: 397–402.
27. Pistis M, Belelli D, Peters JA, Lambert JJ (1997) The interaction of general anaesthetics with recombinant GABAA and glycine receptors expressed in *Xenopus laevis* oocytes: A comparative study. *Br J Pharmacol* 122:1707–1719.
28. Wachowiak M, Shipley MT (2006) Coding and synaptic processing of sensory information in the glomerular layer of the olfactory bulb. *Semin Cell Dev Biol* 17: 411–423.
29. Uludağ K, et al. (2004) Coupling of cerebral blood flow and oxygen consumption during physiological activation and deactivation measured with fMRI. *Neuroimage* 23:148–155.
30. Pasley BN, Inglis BA, Freeman RD (2007) Analysis of oxygen metabolism implies a neural origin for the negative BOLD response in human visual cortex. *Neuroimage* 36:269–276.
31. Hyder F, Rothman DL, Shulman RG (2002) Total neuroenergetics support localized brain activity: Implications for the interpretation of fMRI. *Proc Natl Acad Sci USA* 99: 10771–10776.
32. Maandag NJ, et al. (2007) Energetics of neuronal signaling and fMRI activity. *Proc Natl Acad Sci USA* 104:20546–20551.
33. Smith AJ, et al. (2002) Cerebral energetics and spiking frequency: The neurophysiological basis of fMRI. *Proc Natl Acad Sci USA* 99:10765–10770.
34. Imas OA, Ropella KM, Wood JD, Hudetz AG (2004) Halothane augments event-related gamma oscillations in rat visual cortex. *Neuroscience* 123:269–278.
35. Kroeger D, Amzica F (2007) Hypersensitivity of the anesthesia-induced comatose brain. *J Neurosci* 27:10597–10607.
36. Vanderwolf CH (2000) Are neocortical gamma waves related to consciousness? *Brain Res* 855:217–224.
37. Detsch O, Vahle-Hinz C, Kochs E, Siemers M, Bromm B (1999) Isoflurane induces dose-dependent changes of thalamic somatosensory information transfer. *Brain Res* 829: 77–89.
38. Peeters RR, Tindemans I, De Schutter E, Van der Linden A (2001) Comparing BOLD fMRI signal changes in the awake and anesthetized rat during electrical forepaw stimulation. *Magn Reson Imaging* 19:821–826.
39. Sutton LN, Frewen T, Marsh R, Jaggi J, Bruce DA (1982) The effects of deep barbiturate coma on multimodality evoked potentials. *J Neurosurg* 57:178–185.
40. Doucette W, Restrepo D (2008) Profound context-dependent plasticity of mitral cell responses in olfactory bulb. *PLoS Biol* 6:e258.
41. Kay LM, et al. (2009) Olfactory oscillations: the what, how and what for. *Trends Neurosci* 32:207–214.
42. Scott JW, Scott-Johnson PE (2002) The electroolfactogram: A review of its history and uses. *Microsc Res Tech* 58:152–160.
43. Strowbridge BW (2009) Role of cortical feedback in regulating inhibitory microcircuits. *Ann N Y Acad Sci* 1170:270–274.
44. Shepherd GM, Chen WR, Willhite D, Migliore M, Greer CA (2007) The olfactory granule cell: From classical enigma to central role in olfactory processing. *Brain Res Brain Res Rev* 55:373–382.
45. Raichle ME, Gusnard DA (2002) Appraising the brain's energy budget. *Proc Natl Acad Sci USA* 99:10237–10239.
46. Shulman RG, Hyder F, Rothman DL (2009) Baseline brain energy supports the state of consciousness. *Proc Natl Acad Sci USA* 106:11096–11101.
47. Hyder F, et al. (2001) Quantitative functional imaging of the brain: Towards mapping neuronal activity by BOLD fMRI. *NMR Biomed* 14:413–431.
48. Shulman RG, Hyder F, Rothman DL (2002) Biophysical basis of brain activity: Implications for neuroimaging. *Q Rev Biophys* 35:287–325.
49. Clarke DD, Sokoloff L (1994) Circulation and energy metabolism of the brain. *Basic Neurochemistry*, eds Siegel GJ, Agranoff BW, Albers RW, Molinoff PB (Raven, New York), pp 645–680.
50. Shulman RG, Rothman DL, Behar KL, Hyder F (2004) Energetic basis of brain activity: Implications for neuroimaging. *Trends Neurosci* 27:489–495.
51. Sibson NR, et al. (1998) Stoichiometric coupling of brain glucose metabolism and glutamatergic neuronal activity. *Proc Natl Acad Sci USA* 95:316–321.
52. Buckner RL, Andrews-Hanna JR, Schacter DL (2008) The brain's default network: Anatomy, function, and relevance to disease. *Ann N Y Acad Sci* 1124:1–38.
53. Tian L, et al. (2007) The relationship within and between the extrinsic and intrinsic systems indicated by resting state correlational patterns of sensory cortices. *Neuroimage* 36:684–690.
54. Davison IG, Katz LC (2007) Sparse and selective odor coding by mitral/tufted neurons in the main olfactory bulb. *J Neurosci* 27:2091–2101.
55. Olshausen BA, Field DJ (2004) Sparse coding of sensory inputs. *Curr Opin Neurrobiol* 14:481–487.
56. Mori K, Nagao H, Yoshihara Y (1999) The olfactory bulb: Coding and processing of odor molecule information. *Science* 286:711–715.
57. Cinelli AR, Hamilton KA, Kauer JS (1995) Salamander olfactory bulb neuronal activity observed by video rate, voltage-sensitive dye imaging. III. Spatial and temporal properties of responses evoked by odorant stimulation. *J Neurophysiol* 73:2053–2071.
58. Guthrie KM, Gall CM (1995) Functional mapping of odor-activated neurons in the olfactory bulb. *Chem Senses* 20:271–282.
59. Mackay-Sim A, Shaman P (1984) Topographic coding of odorant quality is maintained at different concentrations in the salamander olfactory epithelium. *Brain Res* 297: 207–216.
60. Wachowiak M, Cohen LB, Zochowski MR (2002) Distributed and concentration-invariant spatial representations of odorants by receptor neuron input to the turtle olfactory bulb. *J Neurophysiol* 87:1035–1045.
61. Shulman RG, Rothman DL, Hyder F (1999) Stimulated changes in localized cerebral energy consumption under anesthesia. *Proc Natl Acad Sci USA* 96:3245–3250.